INTERNATIONAL JOURNAL FOR NUMERICAL METHODS IN FLUIDS
Int. J. Numer. Meth. Fluids 2005; **47**:1027–1034
Published online 27 January 2005 in Wiley InterScience (www.interscience.wiley.com). DOI: 10.1002/fld.883

Adjoint sensitivity analysis for fluid flow with free surface

I. Y. Gejadze*,† and G. J. M. Copeland

Department of Civil Engineering Strathclyde University, 107 Rottenrow, Glasgow G4 0NG, U.K.

SUMMARY

This paper develops the adjoint sensitivities to the free surface incompressible barotropic Euler equations in order to allow for the assimilation of measurements of currents and free surface elevations into an unsteady flow solution by boundary control. To calculate a variation in a surface variable, a mapping is used in the vertical to shift the problem into a fixed domain. Then a variation is evaluated from the Jacobian matrix of the mapping. After calculating a variation in the surface variable and applying the inverse transformation, the tangent linear model is considered in the original space where the adjoint equations are then derived. The method is demonstrated by application to an unsteady flow in an open channel (a 2D vertical section model). A wider application is to the construction of a fully three-dimensional coastal ocean model that allows assimilation of tidal elevation and current data. Copyright © 2005 John Wiley & Sons, Ltd.

KEY WORDS: sensitivity analysis; Euler equations; free surface; adjoint problem

1. INTRODUCTION

The simulation of water circulation in coastal areas requires the application of either two-dimensional (2D) or three-dimensional (3D) computer flow models. These models calculate solutions for either the 2D shallow water equations (SWE) or for the fully 3D non-hydrostatic free surface Navier–Stokes equation (fsNS) in original formulation [1], or in terrain following co-ordinates [2]. All of these calculations require that the solution is driven by an unsteady inflow Dirichlet boundary condition. This condition is not generally known accurately enough and has to be adjusted using the measured data available at scattered locations within the model domain, obtained by current metres and tide gauges, for example. The process of adjustment can be systematized by calculating appropriate sensitivities to guide a gradient

*Correspondence to: I. Y. Gejadze, Department of Civil Engineering Strathclyde University, 107 Rottenrow, Glasgow G4 0NG, U.K.
†E-mail: igor.gejadze@strath.ac.uk

Contract/grant sponsor: The Engineering and Physical Sciences Research Council; contract/grant number: GR/R60881, GR/R60898

Received 27 April 2004
Revised 13 October 2004
Accepted 18 October 2004

descent algorithm. The adjoint sensitivity analysis has been performed for SWE [3], depth-integrated tidal models and for potential flow. Adjoint models developed for oceanographic (deep water) applications, see for example Reference [4], do not determine sensitivities to variations in the free surface and therefore cannot directly assimilate water elevation data (although it can be achieved by introducing the measured geopotential surface). This paper presents the adjoint formulation of the non-hydrostatic barotropic free surface Euler equations (fsE) in 2D vertical section. The method is general and can be extended to the 3D fsNS. The novelty of this work is in the complete treatment of the free surface in the adjoint problem. This is probably the first fsE adjoint model that is free from the hydrostatic assumption in any form and can be used for short waves and in the case of very sharp bed changes.

2. MODEL PROBLEM

Let us consider a 2D free surface inviscid flow in a channel, where the x-axis is directed along the channel, and the y-axis—from the channel bed to the surface. Velocities $u = u(x, y, t)$ and $v = v(x, y, t)$ are associated to x- and y-axes, respectively. The governing equations are as follows:

$$S_t + u(x, S(x,t), t)S_x - v(x, S(x,t), t) = 0 \tag{1}$$

$$u_x + v_y = 0 \tag{2}$$

$$u_t + uu_x + vu_y + p_x = 0 \tag{3}$$

$$v_t + uv_x + vv_y + p_y + g = 0 \tag{4}$$

$$x \in (0, L), \quad y \in (f(x), S(x,t)), \quad t \in (0, T))$$

where $S(x,t)$ is the elevation function describing a free surface, $f(x)$ is the channel bed shape function, such that $f(0) = 0$, p is the relative pressure, $p = (p - p_\infty)/\rho$, p_∞ is the pressure at infinity, $\rho = \text{const}$ is density. Let us denote as $\hat{S}_k =: \hat{S}(x_k, t)$ elevation measurements given at some points $x_k \in (0, L)$; and as $\hat{u}_{l,m} =: \hat{u}(x_l, Y_m, t)$—$u$-velocity measurements at some points $x_l \in (0, L)$ along the trajectories $Y_m =: Y_m(x_l, t) \in (f(x), S(x,t))$. We will use boundary control to assimilate the data given by considering the objective functional

$$J = \frac{1}{2}\sum_k \int_0^T (S(x_k, t) - \hat{S}_k)^2 \, \mathrm{d}t + \frac{1}{2}\sum_l \sum_m \int_0^T (u(x_l, Y_m(x_l, t)) - \hat{u}_{l,m})^2 \, \mathrm{d}t \tag{5}$$

The initial state is assumed to be known and we will consider it, for simplicity, as trivial

$$S(x, 0) = Z, \quad u(x, y, 0) = 0, \quad v(x, y, 0) = 0$$

The open control boundary is assumed at $x = 0$, and the passive boundary at $x = L$. An open boundary is usually introduced when we consider flow in a finite region that is a part of a global flow. Thus, the perfect open boundary condition has to emulate the same flow behaviour within the model domain as if the global model was covered in its entirety. Particularly, it must allow the waves originated within the model domain to pass unhampered through it without reflection. Therefore, Dirichlet condition at the open boundary prescribes an incident

component of state variables that is associated with the incoming characteristics. We use a simple numerical approach described in Reference [5] to distinguish between the incident and reflected parts of the solution. This approach is valid for long-wave cases, assuming there is a pure wave motion at the boundary. We shall denote incident components by the subscript $\rightarrow$, in order to show that they are driving conditions originated from the exterior $x \in (-\infty, 0]$ directed towards the interior. It can be shown that if we assume $S_x(0,t) = 0$, then the only control variable to be found at the control boundary is

$$u_{\rightarrow}(0, y, t), \quad y \in (0, S(0,t))$$

For the reflected component $u_{\leftarrow}(0, y, t) = u(0, y, t) - u_{\rightarrow}(0, y, t), \ y \in (0, S(0,t))$ we use the radiation boundary. By radiation boundary, we mean Sommerfeld condition applied to the outgoing component of u (or u^*) assuming zero surface slope $S_x = 0$ (or $S_x^* = 0$). For the passive boundary $x = L$, we use radiation boundary. For the channel bed, we consider the free slip condition, i.e.

$$u(x, f, t) f_x - v(x, f, t) = 0$$

and for the free surface, we have the dynamic condition

$$p(x, S(x,t), t) = 0$$

We should mention the two assumptions about the surface that are made in the given formulation. The first one is that the free surface can be uniquely described by the graph of $S(x,t)$. Thus, the model cannot cope with such phenomena as breaking waves, for example. Secondly, we use a simplified form of the surface boundary condition neglecting the surface tension.

The main difficulty with the problem of interest consists in deriving the variation in the surface variable $S(x,t)$. A classical procedure is that the variation in a certain dependent variable is calculated assuming all the other dependent variables are simply functions of space and time. Thus, we face a contradiction: in order to calculate the variation in $S(x,t)$, it must be fixed (so as to define $u(x, y, t), v(x, y, t), \ y \in f, S$). A similar difficulty is that the value of the control variable, which is updated in the course of an iterative process $u_{\rightarrow}^{i+1} = u_{\rightarrow}^{i} + \delta u_{\rightarrow}^{i}$ generates a new control domain $y \in (0, S^{i+1}(0,t))$, which is different from the domain $y \in (0, S^{i}(0,t))$ where $u_{\rightarrow}^{i+1}$ is actually defined.

Let us denote $\mathbb{R}[x, y, t]$ the original co-ordinate system and introduce a new co-ordinate system $\mathbb{R}'[x', y', t']$ related to $\mathbb{R}$ by the transformation $\mathbb{Q} : \mathbb{R} \rightarrow \mathbb{R}'$ as follows:

$$t' = t, \quad x' = x, \quad y' = (y - f)/(S - f) \tag{6}$$

assuming $S(x,t) > f(x)$, $\forall x, t$. We can write for derivatives

$$\partial_t = \partial_{t'} - \frac{h_1'}{S - f}\,\partial_{y'}, \quad \partial_x = \partial_{x'} - \frac{h_2'}{S - f}\,\partial_{y'}, \quad \partial_y = \frac{1}{S - f}\,\partial_{y'}$$

where

$$h_1' = y' S_{t'}, \quad h_2' = (1 - y') f_{x'} + y' S_{x'}$$

We can see that the velocities $u'(x', y', t')$ and $v'(x', y', t')$ are defined for all $y' \in (0, 1)$, i.e. $S(x', t')$ is no longer a part of the velocity definition. Therefore, we apply the classical

approach to evaluate the variation in the function $S(x', t')$, which is now explicitly incorporated into the model equations written in the transformed space $\mathbb{R}'$. A similar approach for steady state shape optimization is described in Reference [6]. Also, in $\mathbb{R}'$ the control variable $u'_{\rightarrow}$ can be updated because it is always defined in the same domain. Thus, the control problem may be stated in $\mathbb{R}'$ as a minimization problem for the objective functional J' that is simply (5) reformulated in $\mathbb{R}'$. In fact, both the forward model and the adjoint model could be formulated and resolved in $\mathbb{R}'$. This is often referred to as a problem stated in σ-co-ordinates [2]. In practice, however, many solvers built for oceanographic applications work in $\mathbb{R}$. In order to cope with existing solvers the adjoint equations derived in $\mathbb{R}'$ can be re-formulated back to $\mathbb{R}$ using the transformation $\mathbb{Q}^{-1}$, which is inverse to $\mathbb{Q}$. The control, however, can be correctly exercised only in $\mathbb{R}'$. Therefore, the adjoint variables calculated in $\mathbb{R}$ should be mapped into $\mathbb{R}'$ to serve for control purposes.

The adjoint in $\mathbb{R}$ is as follows:

$$-S_t^* - (u(x,S,t)S^*)_x - S_x u_y(x,S,t)S^* - \mathbb{F} + r_s = 0 \tag{7}$$

$$u_x^* + v_y^* = 0 \tag{8}$$

$$-u_t^* - uu_x^* - vu_y^* - p_x^* - v_y u^* + v_x v^* + 2S_x S^* \delta(y-S) + r_u = 0 \tag{9}$$

$$-v_t^* - uv_x^* - vv_y^* - p_y^* - u_x v^* + u_y u^* - 2S^* \delta(y-S) = 0 \tag{10}$$

$$x \in (0,L), \quad y \in (f,S), \quad t \in (0,T)$$

where

$$\mathbb{F} = \sum_{i=1}^{3} \left[\left(\int_f^S a_{i,1} w_i^* \, \mathrm{d}y \right)_t + \left(\int_f^S a_{i,2} w_i^* \, \mathrm{d}y \right)_x - \int_f^S a_{i,3} w_i^* \, \mathrm{d}y \right], \quad w^* = \{p^*, u^*, v^*\} \tag{11}$$

$$r_u = \sum_l \sum_m (u - \hat{u}_{l,m}) \delta(x - x_l) \delta(y - Y_m)$$

$$r_S = \sum_k (S - \hat{S}_k) \delta(x - x_k) + \sum_l \sum_m [(u - \hat{u}_{l,m}) u_y]_{Y_m} \left(\frac{Y_m - f}{S - f} - \frac{\partial Y_m}{\partial S} \right) \delta(x - x_l)$$

The coefficients in (11) are those obtained when differentiating the governing equations in $\mathbb{R}'$ with respect to S' and then transformed back in $\mathbb{R}$ using $\mathbb{Q}^{-1}$

$$a_{2,1} = 0, \quad a_{2,2} = -y' u_y, \quad a_{2,3} = -(v_y - h_2 u_y)/(S - f)$$

$$a_{3,1} = -y' u_y, \quad a_{3,2} = -y'(u u_y + p_y), \quad a_{3,3} = -(h_0 u_y - h_2 p_y)/(S - f)$$

$$a_{4,1} = -y' v_y, \quad a_{4,2} = -y' u v_y, \quad a_{4,3} = -(h_0 v_y + p_y)/(S - f)$$

where $h_0 = v - h_1 - u h_2$, and $h_1 = \mathbb{Q}^{-1} h_1'$, $h_2 = \mathbb{Q}^{-1} h_2'$. The initial (terminal) and boundary conditions for the adjoint problem are

$$S^*(x,T) = 0, \quad u^*(x,y,T) = 0, \quad v^*(x,y,T) = 0$$

$$u^*(x,f,t) f_x - v^*(x,f,t) = 0, \quad p^*(x,S,t) = 0$$

The radiation boundary for u^* must be used both at $x = 0$ and L.

Let us denote by $\nabla J'[r.]$ the sensitivity on $u'_{\rightarrow}$ generated by a certain residual r, which could be either the r_S source term in (7) or the r_u source term in (9), or both. The corresponding sensitivity expression is as follows:

$$\nabla J'[\cdot] = -S(0,t')[p'^* + u'u'^*]_{x'=0} \tag{12}$$

The sensitivity in (12) is, in fact, a gradient J' on $u'_{\rightarrow}$ and can be used in a gradient optimization algorithm. Studying the sensitivity responses to different sources of information and their combinations is a core application of sensitivity analysis. For example, it allows for questions on the solvability of the problem based on incomplete measurements and on optimal location of the sensors to be clarified.

3. NUMERICAL EXPERIMENTS

A trial numerical implementation was made using a finite-difference semi-explicit solution of the problem with a fixed regular mesh similar to the well-known SOLA algorithm [7]. In solving the forward model, the fields u, v, p and S are saved in the memory. These data are recalled when the TLM or the adjoint problem (7)–(11) is running. In order to underline the general applicability of the method, we designed a special test case in which the bed function suddenly changes from being deep to shallow. In reality, this describes a situation near the 'shelf' edge. This change happens over a one space discretization step, i.e. f_x is always bounded, and the transformation (6) remains well-posed. A particular bathymetry sketch is shown in Figure 1. The numerical experiments carried out here are sometimes referred to as 'identical twin experiments'. Pseudo-residuals r_u and r_S are formed as a difference between the two forward solutions at the measurement points generated by two distinct control inputs that may be interpreted as a 'true value' and an 'initial guess'. These pseudo-residuals are used as driving sources for solving the adjoint problem. The resulting sensitivities, calculated by (12), are then compared to the error function δu that is the difference between these two causal control inputs. In a perfect case, the mismatch has to be infinitesimal. We assume that $u_{\rightarrow}$ is uniform through the depth and varies as follows:

$$u_{\rightarrow}(0,t) = U_0/2(1 + \sin(\pi(3/2 + t/T_0))) \tag{13}$$

where T_0 is the wave period, and U_0 is the amplitude. This function is a lifted sinusoid shown in Figure 2 (left), line 1. The number of grid nodes used is $N_x = 100$ and $N_y = 21$, and the space discretization steps are $\Delta x = L/N_x$ and $\Delta y = Z/N_y$. For a certain set of parameters $L = 2000$ m, $Z = 80$ m, $T = 600$ s, $U_0 = 1$ m/s, $T_0 = 144$ s, $\Delta t = 0.6$ s, we obtain results given in Figure 2 (left). Here, line 2 shows the depth-averaged actual value of $u(0, y, t)$ that is naturally different from the incident one, being a superposition of the incident wave and the wave reflected from the step. The control (13) produces the elevation measurements $\hat{S}_1(t)$ shown in line 3, and the velocity measurements at all grid nodes shown in line 4. We will assume that all these data correspond to a true control input. One can see that the velocity profile at the measurement line $x = \frac{3}{4}L$ is uniform (all the velocity sensors at the different depths display the same value up to $t \approx 450$ s) until the non-uniform velocity field generated near the step has been delivered to the sensors by advective transport. Both $\delta u'$ and $\nabla J'$ are normalized to allow us to compare the shapes. A trivial 'initial guess' is chosen at first,

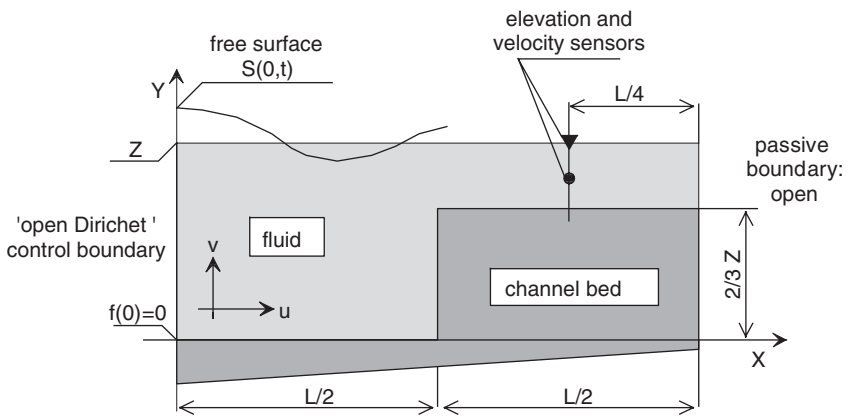

Figure 1. The bathymetry sketch.

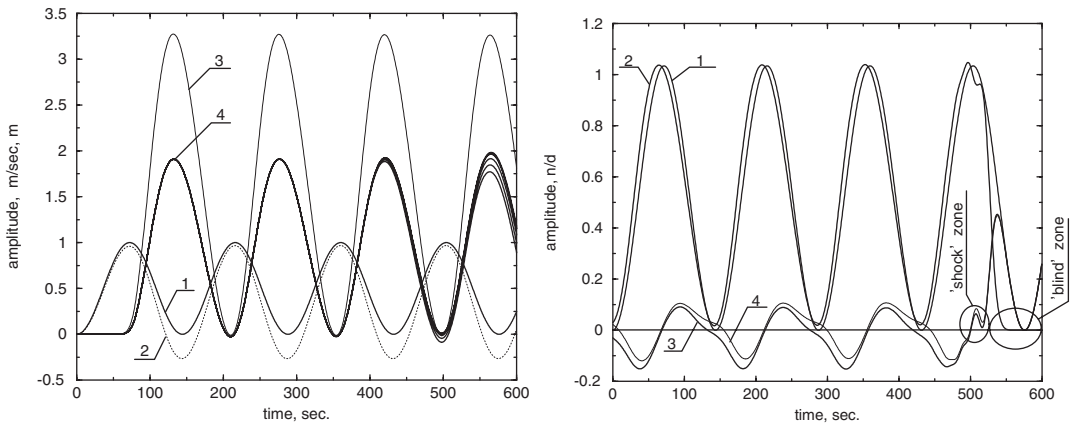

Figure 2. Left: incident input and measurements; right: incident input and sensitivities.

i.e. $u_{\rightarrow}(0, y, t) = 0$, $S_{\rightarrow}(0, t) = Z$. Only one u-velocity sensor located at $y' = \frac{1}{2}$ is used in this example. The results are shown in Figure 2 (right): $\delta u'$—in line 1, $\nabla J'[r_u]$—in line 2, the mismatch $\delta u' - \nabla J'[r_u]$—in line 3, the mismatch $\delta u' - \nabla J'[r_S]$—in line 4. The sensitivities at $x = 0$ are taken at $y' = \frac{1}{2}$, but in the present case they are almost uniform through the depth. After some initial transition period, the mismatch becomes a regular function. This mismatch is mostly due to a non-linear contribution produced by δu. This is proved by the fact that if the pseudo-residuals are generated by the TLM, the regular mismatch becomes an order of magnitude smaller. The remainder may be explained by grid-related numerical effects. For better comprehension we present the patterns of adjoint pressure field generated by the residuals r_u and r_S, which are shown in Figure 3 (left) and Figure 3 (right) correspondingly. In case of trivial initial guess, it is p^* that defines $\nabla J'$ at $x = 0$. When it is driven by r_u, p^* is a discontinuous function of x in the position of δ-source. It can be seen that the wave and

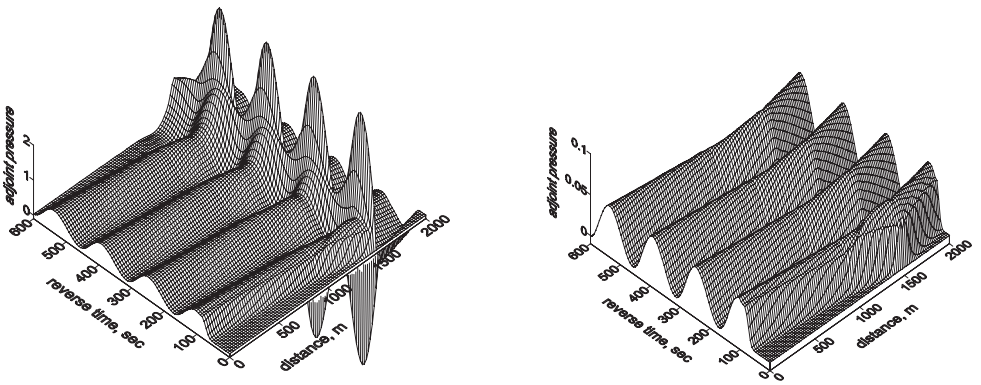

Figure 3. Adjoint pressure field p^* generated by r_u (left) and by r_S (right).

the anti-wave generated by r_u are going in antipodal directions. For a straight channel p^* is a perfectly anti-symmetrical function of x. We can clearly observe the difference in the wave celerity for deep and shallow regions, which occur at $x = 1000\,\text{m}$. When driven by r_S, adjoint fields are continuous, with discontinuity only in $\partial \cdot / \partial x$. Thus, the adjoint solution based on r_S can be obtained on a coarser grid and requires less computational work.

4. SUMMARY

In this paper, we present the continuous (inconsistent) adjoint model for barotropic Euler equations including the free surface. The procedure for deriving the adjoint equations is not trivial. We use a co-ordinate transformation in the vertical to shift the problem into a 'fixed' domain and then derive the variation in the surface variable from the Jacobian of the mapping. We note that although the adjoint problem may be eventually stated and solved in the original space, the control can only be exercised in the transformed space. Another important result indicates that only an incident component of state variables can be controlled. This follows from the predominant hyperbolic behaviour of the problem. The results of numerical experiments have partially validated the theory developed in this paper. A detailed derivation of the adjoint equations, advanced treatment of open boundaries based on the characteristic representation, as well as a number of numerical experiments including 'gradient' test, which validates the accuracy of the sensitivities obtained, should be found in Reference [8].

ACKNOWLEDGEMENTS

The authors are grateful to Dr. Simon Neill, Centre for Applied Oceanography, University of Wales, Bangor, for fsNS solver used as a prototype code and Prof. I. M. Navon, Florida state University, for general guidance and useful discussions.

REFERENCES

1. Casulli V, Zanolli P. Semi-implicit numerical modelling of non-hydrostatic free-surface flows for environmental problems. *Mathematical and Computer Modelling* 2002; **36**:1131–1149.
2. Ezer T, Mellor GL. Simulations of the Atlantic Ocean with a free surface sigma co-ordinate ocean model. *Journal of Geophysical Research* 1997; **102**(15):647–657.
3. Sanders BF, Katopodes ND. Adjoint sensitivity analysis for shallow-water wave control. *Journal of Engineering Mechanics ASCE* 2000; 909–919.
4. Malanotte-Rizzoli P, Tziperman E. The oceanographic data assimilation problem: overview, motivation and purposes. In *Modern Approaches to Data Assimilation in Ocean Modelling*, Malanotte-Rizzoli (ed.). Elsevier: Amsterdam, 1996; 3–17.
5. Copeland GJM. A practical alternative to the mild-slope wave equation. *Coastal Engineering* 1985; **9**:125–149.
6. Jameson A, Martinelli L, Pierce NA. Optimum aerodynamic design using the Navier–Stokes equations. *Theoretical and Computational Fluid Dynamics* 1998; **10**:213–237.
7. Neill SP, Copeland GJM, Ferrier G, Folkard AM. Observations and numerical modelling of a non-buoyant front in the Tay Estuary, Scotland. *Estuarine*, *Coastal and Shelf Science* 2004; **59**:173–184.
8. Gejadze I, Copeland GJM. Open boundary control for Navier–Stokes equations including free surface: adjoint sensitivity analysis. *Journal of Computational Physics* 2005, submitted.

